IEEE Access
Multidisciplinary ⋮ Rapid Review ⋮ Open Access Journal

Received 27 November 2024, accepted 19 December 2024, date of publication 30 December 2024, date of current version 6 January 2025.

Digital Object Identifier 10.1109/ACCESS.2024.3523864

RESEARCH ARTICLE

Evaluation of Machine Learning Algorithms for NB-IoT Module Energy Consumption Estimation Based on Radio Channel Quality

DUSAN BORTNIK, VLADIMIR NIKIC, SRDJAN SOBOT, DEJAN VUKOBRATOVIC, (Senior Member, IEEE), IVAN MEZEI, (Senior Member, IEEE), AND MILAN LUKIC, (Member, IEEE)
Faculty of Technical Sciences, University of Novi Sad, 21000 Novi Sad, Serbia

Corresponding author: Milan Lukic (milan_lukic@uns.ac.rs)

This work was supported in part by the Ministry of Science, Republic of Serbia, ''Scientific and Artistic Research Work of Researchers in Teaching and Associate Positions at the Faculty of Technical Sciences, University of Novi Sad'' under Project 451-03-65/2024-03/200156; in part by the Science Fund of the Republic of Serbia, through the project REmote WAter quality monitoRing anD INtelliGence–REWARDING, under Grant 6707; and in part by the Horizon 2020 Research and Innovation Staff Exchange under Grant 101086387 (Remarkable).

ABSTRACT In this study, we propose a method to estimate energy consumption in battery-powered Narrowband Internet of Things (NB-IoT) devices using the statistical data available from the NB-IoT modem, thereby circumventing the need for additional circuitry to measure battery voltage or current consumption. A custom edge node with an NB-IoT module and onboard current measurement circuit was developed and utilized to generate a labeled dataset. Each data point, generated upon UDP packet transmission, includes metadata such as radio channel quality parameters, temporal parameters (TX and RX time), transmission and reception power, and coverage extension mode. Feature selection through variance and correlation analysis revealed that coverage extension mode and temporal parameters significantly correlate to the energy consumption. Using these features, we tested 11 machine learning models for energy consumption estimation, assessing their performance and memory footprint, both of which are critical factors for resource-constrained embedded systems. Our best models achieved up to 93.8% of fit with measured values, with memory footprints below 100 KB, some as low as 3 KB. This approach offers a practical solution for the energy consumption estimation in NB-IoT devices without hardware modifications, thereby enabling energy-aware device management.

INDEX TERMS NB-IoT, energy consumption estimation, LPWAN, machine learning.

I. INTRODUCTION

In massive Internet of Things (IoT) applications and scenarios, featuring multiple thousands of edge devices, some of the key concepts affecting scalability and sustainability concern choosing a proper power source. According to [1], by the end of 2024, the number of connected IoT devices has grown 13% over the previous year. Moreover, it is estimated that this number may reach 40 billion by 2030, underscoring the need for sustainable solutions in energy management and connectivity for widespread IoT deployment.

Lithium-thionyl chloride batteries [2] are a choice widely utilized in low-power IoT devices due to their desirable properties such as high energy density, long shelf life, stable voltage output, wide operating temperature range, safety features, minimal maintenance, and overall suitability. However, such batteries feature a very flat discharge curve (Fig. 1), delivering a constant output voltage until almost complete discharge. This property makes it practically impossible to estimate the amount of energy left based on output voltage

The associate editor coordinating the review of this manuscript and approving it for publication was Fan-Hsun Tseng.

measurements, unlike other battery technologies such as Li-ion.

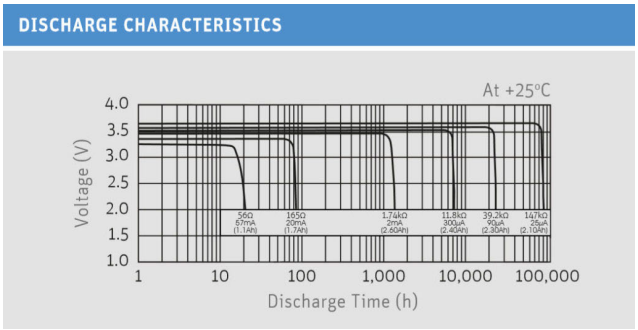

FIGURE 1. Discharge curves of lithium-thionyl chloride batteries [2].

The energy consumption of embedded devices, particularly those utilized for battery-powered telemetry IoT applications, is characterized by aggregating consumption from multiple sources. Certain components exhibit constant energy consumption, while others display variable consumption patterns. These variations can be attributed to a variety of environmental factors, such as temperature and pressure, among others. However, for communication modules particularly, which are commonly integral parts of embedded devices, the radio channel quality parameters emerge as critical determinants of energy consumption variability. As a consequence, developing a robust mechanism for precise estimation of energy consumption of communication modules is necessary for the efficient management of IoT devices and their batteries.

In this study, we investigate the energy consumption characteristics of Narrowband Internet of Things (NB-IoT) communication modules. NB-IoT represents an enhancement to the 4G LTE standard [3], facilitating connectivity for up to 50,000 low-power devices to a single base station. This technology is specifically optimized for low-power devices, enabling a projected battery lifespan of up to ten years. The trade-off for this extended battery life is a reduced data transmission rate; however, a significant advantage of NB-IoT is its extended coverage leading to superior indoor penetration capability, allowing devices to maintain communication with base stations from locations that may be inaccessible to other wireless technologies.

The communication module utilizing NB-IoT is characterized by three distinct coverage extension modes, which operate based on the radio channel quality parameters specific to a given location. These variations in radio channel quality result in corresponding differences in energy consumption. Consequently, the accurate prediction of energy consumption for embedded devices, along with the estimation of their battery lifespan, becomes critical within the context of NB-IoT applications.

Embedded devices utilizing NB-IoT communication modules occasionally exhibit significant energy consumption patterns, particularly during initial network connection procedures. The initial setup necessitates a prolonged and power-intensive connection to the network. However, subsequent activations during which a device wakes up from Power Saving Mode entails a markedly shorter and lower power-consuming reconnection process. Consequently, the predominant contributor to the energy expenditure of these modules is the data transmission activity. This transmission is characterized by various radio channel quality parameters that are relevant during the communication process, in addition to radio channel-independent communication parameters intrinsic to the module's operation. These parameters form the foundational basis of our study, serving as critical input variables for our energy consumption estimation models.

Traditional methods for estimating device's energy consumption and battery lifespan typically rely on measurements of battery voltage and current or analytical modeling of energy consumption associated with communication protocols. In contrast, our approach leverages machine learning (ML) algorithms, which have gained traction in embedded systems with the development of TinyML concepts [4], [5]. The application of ML algorithms enables the creation of models that can derive custom logic to predict specific values based on provided inputs. In this study, we utilize multiple ML algorithms to develop models for predicting energy consumption based on radio channel quality and communication parameters for each transmitted packet. Our main objective is to demonstrate that the energy consumption of communication modules per packet transmission can be estimated using these parameters with high accuracy. We apply different regression-based ML models to predict the energy consumption of transmitting a single packet.

The main contributions of this work are the following:

- a custom dataset comprising 5,880 data points, which includes radio and temporal parameters for each packet, as well as the corresponding amount of consumed energy;
- a comprehensive analysis of 17 dataset features and their mutual correlation;
- a detailed feature reduction analysis based on correlation heatmap and K-best algorithms resulting in numerous feature combinations;
- an in-depth analysis of energy consumption estimation using various regression models, on proposed feature combinations;
- a successful estimation of energy consumption for a transmitted packet with the accuracy of up to 93.8% R2 value utilizing Random Forest regression;
- results showed that temporal parameters (RX time and TX time) carry more information necessary for energy consumption prediction than all radio channel quality parameters combined.

The paper is organized as follows. After the introduction part, in Section II, we provide a comprehensive analysis of related work in this field. In Section III, the hardware architecture used in this study is described in detail.

Section IV covers an explanation of the utilized experimental setup, the creation of the corresponding dataset, and the energy consumption measurement technique. In Section V, a detailed analysis of input features is provided. The next section, Section VI, gives a methodology used for the input feature selection. Subsequently, in Section VII, we describe regression models and corresponding metrics used in this study. In Section VIII, a detailed analysis of results is conducted. Finally, Section IX concludes the paper with a summary and suggestions for the future research area.

II. LITERATURE OVERVIEW

Several studies have emerged focusing on the analysis of NB-IoT network power and energy consumption to predict battery lifespan [6], [7], and [8]. Most of these studies aimed to dissect the operation of NB-IoT modems, to independently analyze each phase and determine the relationship between consumption and various radio channel and temporal parameters. A recent, comprehensive survey addressing the NB-IoT technology efficiency and challenges in terms of energy consumption is presented in [9]. The paper [10] surveys energy-saving strategies for 3GPP-based Cellular IoT, analyzing techniques like parameter configuration and software adjustments to enhance device battery lifetime. Key factors affecting energy use are discussed such as data frequency and DRX cycles. Another study by Yang et al. is focused on the analyses of the energy consumption of NB-IoT in the wilderness [11].

In our paper [12] we presented our custom-designed NB-IoT platform for fine-grained measurements of energy consumption of an NB-IoT module across different phases during the data transmission. Using the designed platform in a real-world setup supported by a mobile operator, we presented several numerical examples of NB-IoT module energy consumption under various settings, in which the energy consumption is decomposed and analyzed across different data transmission phases, resulting in precise phase-by-phase energy consumption measurements.

Apart from analyzing the power and energy consumption of modems, there have been attempts to define energy consumption analytical models that can be used in the estimation of the battery lifespan of a device. The following studies provide both analytical and empirical models to estimate battery lifetime in NB-IoT networks. However, none of them employ ML approaches to accomplish this task.

A. ANALYTICAL AND EMPIRICAL APPROACHES TO THE ENERGY CONSUMPTION ESTIMATION

The first research on reducing NB-IoT energy consumption is based on random access reduction [13]. It utilizes deep uplink packet inspection, and accordingly, pre-assigns radio resources. Furthermore, study [14] introduces mechanisms that leverage the stationary and periodic characteristics of NB-IoT devices that have been demonstrated to reduce energy consumption by as much as 37.8%. Additionally, another paper that provides an analysis and energy optimization of downlink traffic using particle swarm optimization (PSO) was presented in [15].

The first paper estimating the power consumption of a commercially available NB-IoT device introduced an empirical approach [16]. The authors compare their measurements with the results obtained during the 3GPP standardization, demonstrating promising outcomes, as the battery lifetime is only around 10% shorter than the estimates provided by 3GPP.

An analytical model based on Markov Chains is introduced and validated in the different approach by the same authors [17]. The comparison between the proposed model and measurements obtained using an experimental setup consisting of a base station emulator and commercially available NB-IoT devices with a power analyzer is conducted in terms of estimated battery lifetime. The results indicate that their analytical model performs well, with a maximum relative error of 21% in battery lifetime estimation compared to the measurements, assuming an Inter-Arrival Time (IAT) of 6 minutes.

The study given in [18] presents an empirical analysis of NB-IoT technology in a well-designed experimental setup. Authors observed that the main factors determining energy consumption are: module type, network operator, signal quality, usage of energy saving enhancements such as RAI and eDRX. Additionally, the packet size has a negligible effect on overall device power consumption under normal operating conditions.

In [19], the authors conduct a thorough investigation of energy consumption profiling in NB-IoT networks using the Quectel BG96 module across various states of the Radio Resource Control (RRC) protocol. Unlike this paper, they utilized a power analyzer to measure current and voltage. The authors reported that their proposed model accurately depicts the baseline energy consumption of an NB-IoT radio transceiver, with an evaluation error ranging between 0.33% and 15.38%.

Another work presents a comprehensive power consumption model for estimating battery lifetime in two cellular IoT technologies: NB-IoT and Long-Term Evolution for Machines (LTE-M), achieving a modeling inaccuracy within 5% [20]. Similarly to the papers mentioned before, the authors employ a strictly analytical approach to develop the model. However, to estimate battery lifetime, they provide a detailed methodology that considers various configurations of traffic profiles, coverage scenarios, and network parameters.

Recently, an analytical model based on UE power consumption is presented [21]. Using a probabilistic model and simplified state diagram of the NB-IoT device the authors achieved a simulated target battery lifetime of over 11 years with IAT set to 11h.

A paper reporting a custom measurements device (data concentrator) uses 4 radio channel quality parameters (RSRP, RSRQ, RSSI, and SINR) [22]. They are used to evaluate the NB-IoT and LTE link states and select the better one. There are no power or energy estimations in this work.

Recently, a detailed NB-IoT energy consumption profile has been presented based on power meter measurement on Quectel's BG96 module [23]. The energy consumption model is based on TR 45.820 by 3GPP [24]. In [25], the authors analyze the power consumption of the Quectel BG77 module and present an analytical model for battery lifetime estimation.

In a recent study, two parameters are identified as a main contributor to power consumption. Optimizations of NB-IoT transmit power level and the number of independent transmissions sent per day may lead to battery lifetime enhancement [26].

Another paper [27] presents a comprehensive analysis of Qualcomm's NB-IoT modem, detailing the reverse-engineering process used to decode essential frame information and examining various network configurations that influence performance. The study also presents a large NB-IoT dataset, collected from a metropolitan network, and utilizes ML techniques to identify critical factors contributing to low throughput and prolonged delays.

B. ML-BASED APPROACHES TO THE ENERGY CONSUMPTION ESTIMATION

There have been attempts to estimate battery lifespan utilizing ML models, but to the best of our knowledge, no studies have been published on the topic of estimation of power or energy consumption for NB-IoT modems based on ML models. Nevertheless, there have been publications that deal with the same topic in other wireless technologies.

One of them is study [28] which investigates the prediction of the lifetime of a wireless sensor network utilizing LoRa Ra-01 wireless modules. The authors employed a probabilistic framework, developing a model based on Markov chains to estimate the system's lifetime as a function of the data transmission probability throughout the day.

In [29], the authors aim to estimate the battery life of intelligent roadside units using the RSSI parameter, specifically within a GSM technology framework. They provide a detailed description of the test environment setup and the devices used for data acquisition. Various ML models were employed, tested on the collected data, and subsequently compared using the coefficient of determination. They show that the Random Forest regression models were the preferable option for predicting power consumption with an R2 coefficient of 98%.

Energy consumption estimation of IEEE 802.15.4 network transmissions have been studied in [30]. Authors applied various regression-based ML models, such as: linear, gradient boosting, random forest, and deep learning. Results show that deep learning achieves up to 98% accuracy for energy consumption predictions. As inputs for their ML models, authors utilize communication parameters like transmission power, packet size, etc.

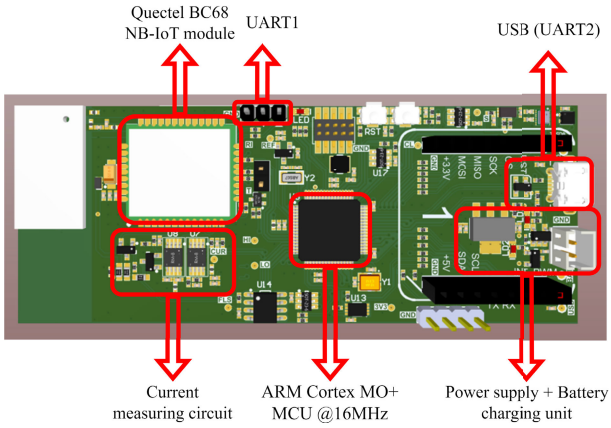

FIGURE 2. Hardware architecture of the edge device.

Authors in [31] used various ML models and LoRa technology to estimate factors other than power consumption, based on numerous radio channel quality parameters. They discovered a correlation between the RSSI parameter and soil humidity values collected from sensors and proposed an ML model for its estimation.

Finally, in paper [32], an ML-based approach for forecasting the resulting uplink transmission power used for data transmissions (over LTE-Advanced) based on the available passive network quality indicators and application-level information was proposed. Employed ML models in this work are: random forest, ridge regression, and deep learning, where random forest performed the best, with a mean average error of 3.166 dB.

A comprehensive overview of LPWAN technologies is presented in [33], where the authors conduct a real-world performance evaluation based on coverage parameters, path loss, packet delivery rate, latency limits, and power consumption. The study highlights that LoRaWAN and Sigfox technologies are more battery-efficient compared to NB-IoT. Additionally, it demonstrates that depending on signal quality, latency can vary significantly, leading to a critical degradation in battery life efficiency within NB-IoT networks.

In recent years, there have been various studies on estimating the capabilities of Li-Ion batteries based on different input features such as voltage, current, or temperature [34]. To achieve this task, some of them utilize different ML techniques such as [35], [36], and [37].

Still, to the best of our knowledge, no published work utilized ML algorithms to estimate energy consumption based on radio channel quality parameters as input features for NB-IoT network technology.

III. EXPERIMENTAL HARDWARE MODULE OVERVIEW

In the context of data collection and dataset development, we utilize a prototype of an edge node device designed

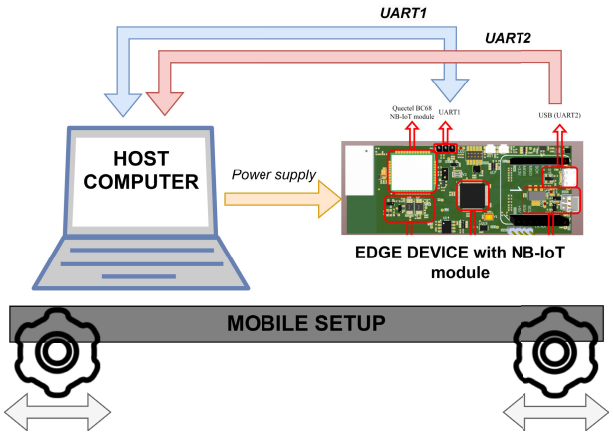

FIGURE 3. An experimental setup used in this study.

for our NB-IoT testbed, as described in our previous publications [12], [38], and [39]. The device architecture, illustrated in Fig. 2, features a BC68 NB-IoT modem from Quectel, and a current measuring circuit. Apart from that, the board is equipped with a 16MHz ARM Cortex M0+ microcontroller unit (MCU).

The device facilitates the transmission of diverse data streams through two distinct serial communication lines. The first serial port is employed for onboard microcontroller logging, capturing essential data pertaining to the most recent packet transmission acquired from the NB-IoT module through AT commands. The second serial port enables the tracking of current consumption patterns, measured for the NB-IoT modem only.

To measure the current consumption of the network modem, a specialized onboard current measuring circuit was implemented. This circuitry is capable of measuring the module's current consumption in both the mA and μA ranges, making it convenient for power analysis during both the NB-IoT module's active periods and Power Saving Mode.

In contrast to the experimental setups in other studies [18], [19], and [29], which utilize external power measuring equipment and similar approaches, our onboard circuit provides a significant advantage for evaluating power performance in large-scale edge node deployments.

IV. DATASET

Utilizing the aforementioned hardware architecture, we developed firmware specifically for dataset generation. This application was designed to execute a sequence of data transmissions, relay modem statistics and information, and continuously measure current consumption. Both sets of information were transmitted to the host computer, where they were parsed and stored in dedicated log files. Subsequent post-processing was necessary to correlate and extract the required data points. In this section, we provide a detailed description of the dataset creation process.

A. EXPERIMENTAL SETUP

To ensure the resulting dataset encompassed diverse radio conditions, our experimental setup was designed to be mobile and battery-powered, allowing measurements to be conducted at various locations without the loss in precision. The setup included a laptop and an edge node device connected via two serial ports. These ports facilitated the separate transfer of current consumption data every millisecond and modem information following each data transmission. The configuration of the setup is illustrated in Fig. 3.

The experiment was designed to collect data from various locations within the Science and Technology Park in Novi Sad, Republic of Serbia. Spanning five floors, from the ground level to the fourth floor, measurement locations were spaced approximately 3.5 meters apart and situated in the building's corridors, as illustrated in Fig. 4.

B. DESCRIPTION AND SIZE OF DATASET

The dataset comprises data points that encapsulate all available information about individual data transmissions utilizing the UDP protocol. As previously described, the experimental setup was positioned at various locations to conduct a sequence of transmissions. This sequence involved ten repetitions for each of four different packet sizes: 16, 32, 64, and 128 bytes. Given that there were 10, 34, 34, 34, and 35 locations per floor, respectively, the resulting dataset comprises a total of 5,880 data points.

Each data point in the dataset contains two pieces of positional information along with the size of the transmitted packet:

- **floor**: Number of the floor at which the experiment was conducted.
- **packet_size**: Size of the packet in bytes.
- **position**: ID of measurement position.

Apart from the floor level, location identification number, and packet size, the data point also consists of information provided by the modem about the transmission itself. In the case of Quectel's BC68 module, this information can be obtained by *AT+NUESTATS* [40] command. The following list describes all available information for each data point in more detail:

- **ecl**: *Enhanced Coverage Level*, which corresponds to 3GPP *Coverage Extension Mode* value for serving cell where 0 indicates excellent conditions, 1 represents good, and 2 moderate or poor conditions.
- **mac_dl/mac_ul**: *Medium Access Control Downlink/Uplink*, representing physical layer throughput (downlink/uplink) in bits-per-second.
- **rlc_dl/rlc_ul**: *Radio Link Control Downlink/Uplink*, representing the RLC layer throughput (downlink/uplink) in bits-per-second.
- **rsrp**: *Reference Signal Received Power*, representing the received power level of the reference signals from the cell.

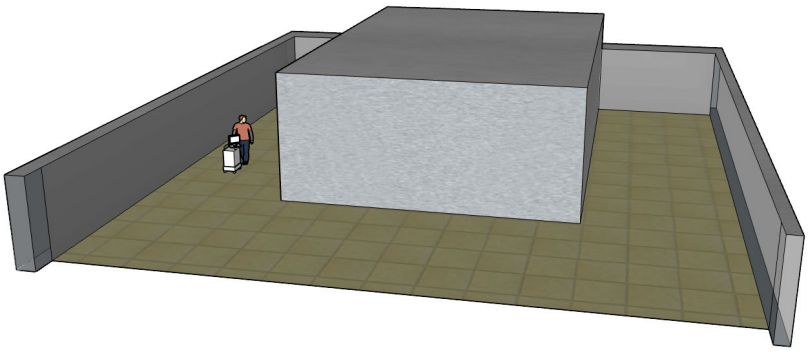

(a) Simplified three-dimensional perspective of the experimental setup.

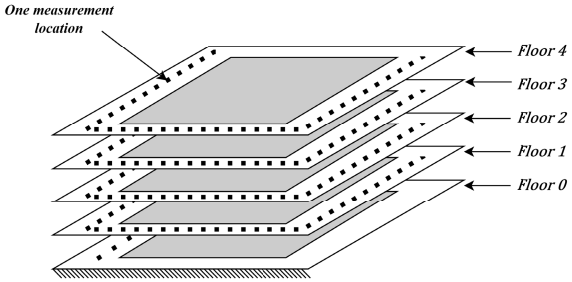

(b) Floor Plan of the building.

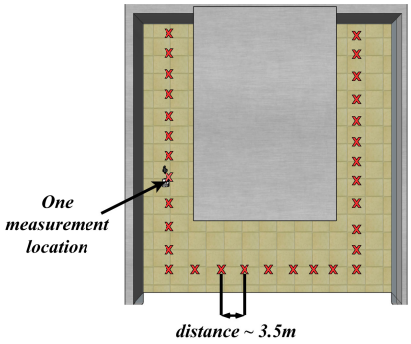

(c) Top view of the floor showing the layout of measurement locations and the distance between each.

FIGURE 4. An experimental scenario used in this study.

- **rsrq**: *Reference Signal Received Quality*, indicating the quality of the received reference signals in centibels.
- **rssi**: *Received Signal Strength Indicator*, representing the overall received signal strength, including the contribution of the serving cell and interference.
- **rx_time**: Total time the device has spent in the receiving state (listening for incoming data) in milliseconds.
- **signal_power**: Strength of the received signal in centibels.
- **snr**: Signal to noise ratio.
- **tx_power**: Power level at which the device is transmitting data in centibels.
- **tx_time**: Total time the device has spent transmitting data in milliseconds.

In addition to the parameters described, each data point also contains information regarding the energy consumption (expressed in milliwatt-hours (mWh)) of the network module, which is derived from accurate onboard measurements.

C. ENERGY CONSUMPTION MEASUREMENTS

Having described all the parameters available for energy consumption estimation, we will now detail the procedure used to measure and associate energy consumption with each transmission. As previously mentioned, the edge node is equipped with an onboard circuit for current consumption measurement, which records the current consumed every millisecond. This value is scaled in the firmware and transmitted as a sample via UART2 (as depicted in Fig. 3). Consequently, a log is created for each location that contains a sequence of consumption measurement samples, as illustrated in Fig. 5a. Furthermore, Fig. 5b provides a visual representation of the consumption log for an individual packet.

To distinguish between transmissions, we implemented a mechanism that sends a special, negative sample value as a separator before each packet is transmitted. This allows us to accumulate samples between two separators, or between a separator and the end of the log, to calculate the electric charge consumption per transmission. Although we are fundamentally calculating electric charge consumption, measured in Coulombs (C), we use milliampere-hours (mAh) as the unit, as it more effectively represents battery consumption. Finally, we multiply the electric charge consumption with the battery voltage (3.7V), to get energy consumption represented in milliwatt-hours (mWh). That being said, the energy consumption can be expressed as the sum of current samples between two separators multiplied by a constant.

V. INPUT FEATURE ANALYSIS

Section IV-B provides a comprehensive overview of the radio channel quality parameters included as input features in the

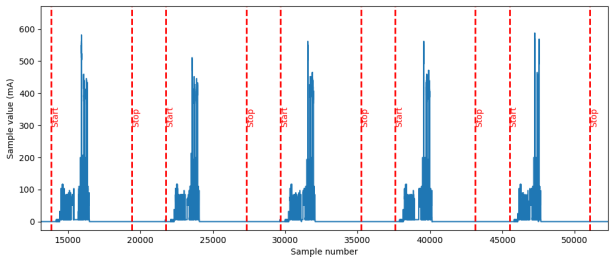

(a) Consumption log for the sequence of packets.

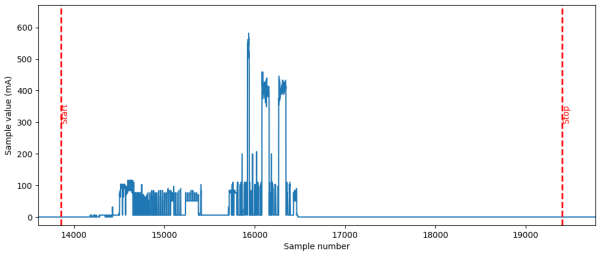

(b) Consumption log for an individual packet.

FIGURE 5. Consumption logs displaying current measurements per packet.

ML models. The following sections outline the analyses conducted on the data collected for each parameter. First, a variance analysis is performed to evaluate the diversity within the dataset for each parameter. This is followed by an examination of the correlation between each parameter and the corresponding energy consumption values.

A. VARIANCE ANALYSIS

The initial step in the analysis of parameter variances involves identification and exclusion of parameters that are irrelevant to the experiment. Consequently, we exclude parameters position and floor level from further analysis to avoid basing our prediction on spatial parameters.

The remaining parameters exhibit significant variability, as illustrated in Fig. 6. Similar, yet more comprehensive analyses of various parameter relationships, including RSRP, CE mode, TX Power, SNR, and throughput for both uplink and downlink stages, are presented in [41].

RSSI and RSRP exhibit a strong correlation, which aligns with expectations given their similar nature in signal strength measurement. On the other hand, TX Power displays a markedly uneven distribution, with approximately 85% of all recorded values converging to a 23dB, which is maximum value for TX power. This also aligns with the conclusions drawn in [41]. Additionally, Signal Power is also correlated with both RSSI and RSRP. The CE mode parameter predominantly takes the value 0 in approximately 70% of cases, indicating better signal conditions, while the remaining 30% corresponds to value 1, reflecting poorer coverage conditions.

Time intervals for transmission (TX time) and reception (RX time) show diversity, with the reception time interval rarely repeating. In contrast to the RX time intervals, which exhibit infrequent repetition, the TX time intervals, in some cases, repeat hundreds of times for specific values.

B. ENERGY CONSUMPTION CORRELATION WITH RADIO CHANNEL QUALITY PARAMETERS

After analyzing the variance of the parameters, we examine their correlation with the energy consumption. Fig. 7 presents the distribution of packets in relation to radio channel parameters and energy consumption. The figures in the first and the third row illustrate the distribution of packets based on a specific parameter and consumption, with lighter regions indicating higher density and darker regions indicating lower density. The figures in the second and the fourth row depicts the distribution of packets according to the specific parameter and consumption, in relation to the packet's CE mode. Lighter dot-shaped markers represent packets with CE mode 0, while darker x-shaped markers denote those with CE mode 1.

Fig. 7a and 7d demonstrate that an increase in packet size does not lead to higher energy consumption. This finding aligns with the conclusion presented in [18] that, under normal operating conditions, the size of the packet has a minimal effect on the overall consumption. However, a strong correlation exists between CE modes and consumption, which is consistently observed across other figures as well.

A strong correlation between temporal parameters and energy consumption is evident in Fig. 7g and 7h. The near-linear dependency observed in these figures suggests that these parameters may be the most significant factors in estimating energy consumption.

VI. FEATURE SELECTION

As previously discussed, the generated dataset encompasses a wide range of features. In certain cases, pairs or groups of features exhibit similar patterns, often due to underlying similarities in the information they convey. To mitigate redundancy among input features in machine learning models, we apply feature selection techniques. Numerous methods are available for this purpose, as outlined in comprehensive reviews [42], [43], and [44].

The following sections describe the methodology for selecting an optimal subset of input features. This process employs two distinct approaches: Feature correlation heatmap analysis, which quantitatively assesses the correlations between parameters and organizes them based on their similarity, and K-Best Feature Selection, which numerically identifies combinations of a specified number of input features that optimize performance according to various target functions. In our study, we employed the Scikit-learn [45] and Tensorflow [46] frameworks to address this task.

A. FEATURE CORRELATION HEATMAP

A correlation heatmap provides a visually intuitive approach to illustrating the relationships between features within a dataset. At its core is the correlation coefficient, a statistical

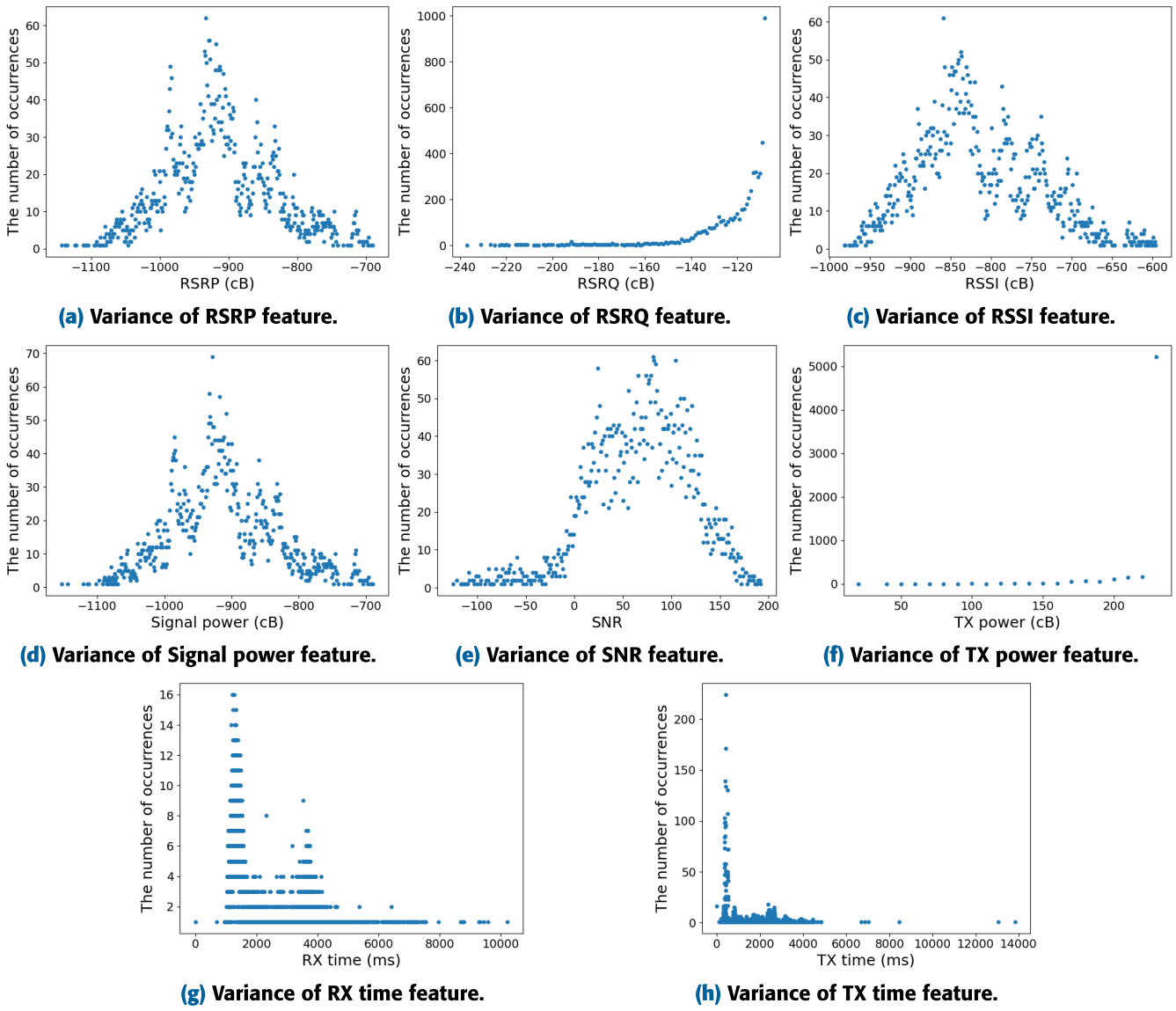

(a) Variance of RSRP feature. (b) Variance of RSRQ feature. (c) Variance of RSSI feature.

(d) Variance of Signal power feature. (e) Variance of SNR feature. (f) Variance of TX power feature.

(g) Variance of RX time feature. (h) Variance of TX time feature.

FIGURE 6. Variances of selected input features.

measure that quantifies the strength and direction of the linear relationship between two variables. The values of the correlation coefficient range from −1 to 1, where:

- 1 signifies a perfect positive correlation;
- −1 signifies a perfect negative correlation;
- and 0 indicates no correlation between the variables.

Fig. 8 presents a heatmap illustrating the correlation between parameters. The correlation calculation method used in the displayed heatmap is the standard Pearson correlation coefficient. The presence of high values indicates a strong correlation between two or more parameters. This finding can be leveraged to reduce the number of input features in ML models by grouping correlated parameters, as shown in Table 1. Based on these groups, all possible parameter combinations can be calculated. As *Group1*, *Group2*, *Group3* and *Group4* consist of 3, 2, 3, and 2 members, respectively, there are *36* possible input parameters combinations.

TABLE 1. Groups of parameters sorted by feature correlation heatmap analysis.

Independent	Group 1	Group 2	Group 3	Group 4
packet_size	rsrp	rsrq	tx_time	rlc_ul
rlc_ul	rssi	snr	rx_time	mac_dl
mac_ul	signal_power		ecl	
tx_power				

The correlation between parameters within the same group is evident in the variance graphs. For instance, Fig. 6c, 6a and 6d display significant similarities, which is expected given their interdependence as radio channel quality parameters. Consequently, reducing the number of input

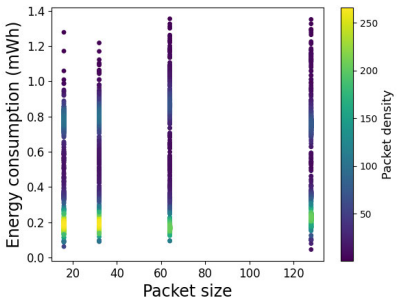

(a) Packet density by size and consumption.

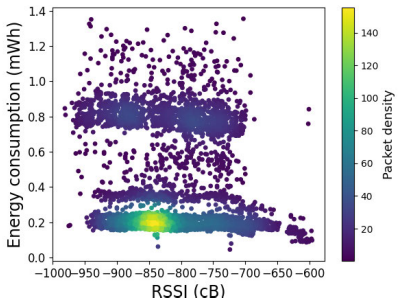

(b) Packet density by RSSI and consumption.

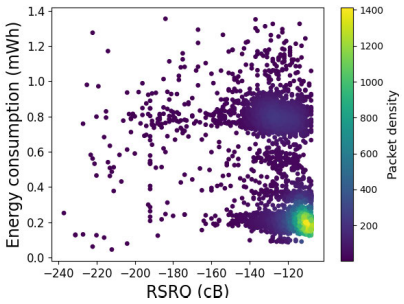

(c) Packet density by RSRQ and consumption.

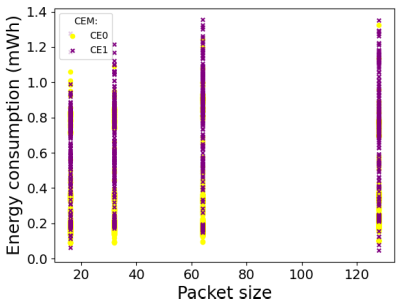

(d) Distribution of energy consumption per packet depending on packet size and CE mode.

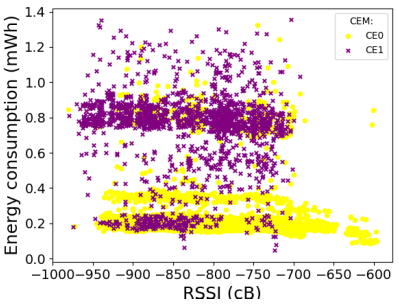

(e) Distribution of energy consumption per packet depending on RSSI and CE mode.

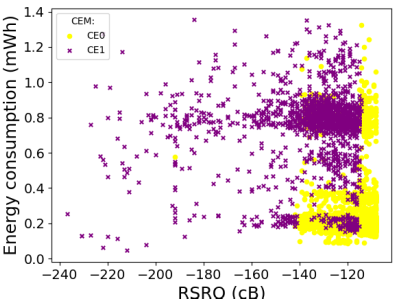

(f) Distribution of energy consumption per packet depending on RSRQ and CE mode.

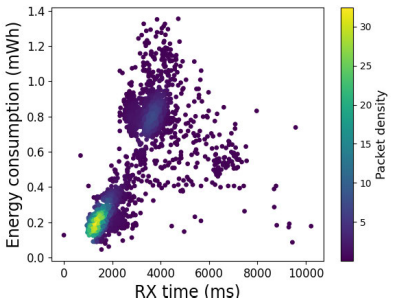

(g) Packet density by RX time and consumption.

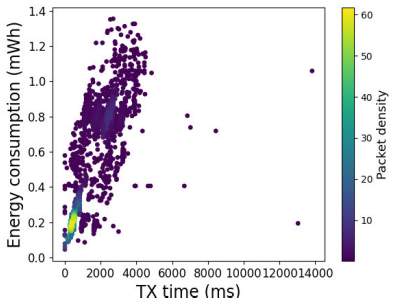

(h) Packet density by TX time and consumption.

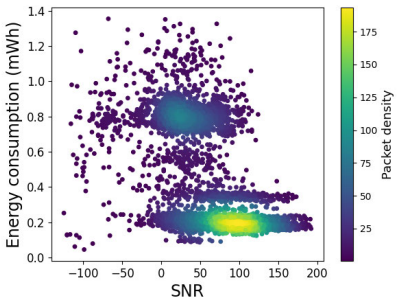

(i) Packet density by SNR and consumption.

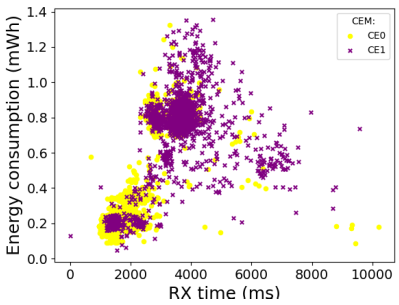

(j) Distribution of energy consumption per packet depending on RX time and CE mode.

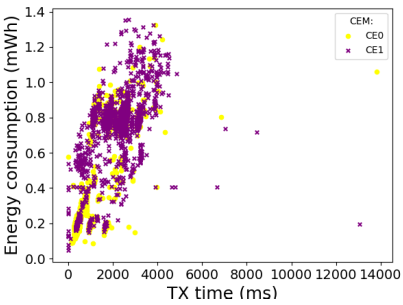

(k) Distribution of energy consumption per packet depending on TX time and CE mode.

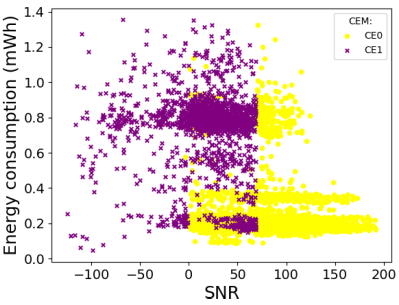

(l) Distribution of energy consumption per packet depending on SNR and CE mode.

FIGURE 7. Packet distribution by radio channel quality parameters and energy consumption.

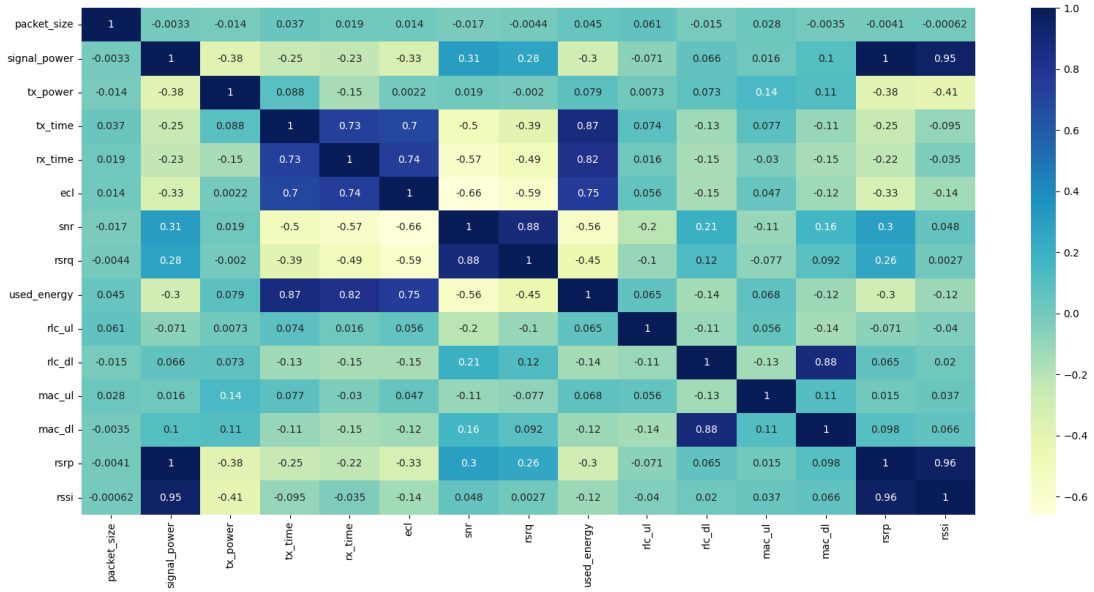

FIGURE 8. A correlation heatmap of input features.

features in ML models can theoretically be accomplished by selecting a single representative parameter from each group, without a substantial loss of accuracy.

Another notable conclusion that applies to the correlation heatmap is that independent parameters introduce small, and in some cases negligible,[1] influence on the prediction result [42]. This can also be seen from Fig. 8, where all independent parameters have weak correlation with the output value in contrast to mutually correlated values, that are members of specific groups. Therefore, apart from the combinations described above, another set of possible combinations that excludes independent parameters is created in order to support this assumption.

B. K-BEST

K Best feature extraction is a filter-based feature selection technique that ranks all the input features based on their relevance to the target variable and selects the top K features which combination yields the highest scores. Scores are calculated based on target functions, which are, in the case of this study:

- *R Regression* – target function that is based on the calculation of Pearson's r-value for each feature and the target.
- *F Regression* – target function, derived from R regression, that calculates the F-value instead of Pearson's r-value.
- *Mutual Info Regression* – target function that computes mutual information between two random variables, thus measuring their dependency.

[1]In our dataset, tx_power has a negligible influence on the power consumption as it is almost always set to the maximum value. However, in a different setting where it may vary significantly, this particular feature would most likely not fall into independent group.

For each target function, different numbers of input features are selected using the K-Best procedure. The number of features is determined based on the size of the input feature sets derived from the feature correlation heatmap analysis procedure, as explained in the section VI-A. Accordingly, the top 8, 6, and 4 input features with the highest scores for each target function, are selected.

The resulting input feature combinations are presented in Table 2. The first four rows represent the selected feature groups of the best four parameters for each target function, the first six rows represent groups of the best six parameters for each target function, and all eight rows represent full feature groups of the best eight parameters for each target function.

C. CUSTOM COMBINATIONS

At last, we also tried some of the custom feature combinations we empirically determined during the initial experimental phase of our research, which we compared with the outputs of the feature selection methods outlined in subsections VI-A and VI-B. The list of these combinations is presented in Table 3.

VII. MODELS OVERVIEW

This section provides a detailed description of the models used in this experiment. Furthermore, it explains the metrics used to evaluate the results, providing insights into their relevance and how they are applied to assess the model's performance.

A. DESCRIPTION OF MODELS AND THEIR PARAMETERS

In this experiment, 11 models are employed to estimate energy consumption. To determine the relationship between a dependent variable – energy consumption and multiple independent variables – radio channel quality parameters

TABLE 2. Feature combinations generated by K-best algorithm.

No.	Combinations					
	KB_FR	KB_RR	KB_MI	KB_FR_NT	KB_RR_NT	KB_MI_NT
1	tx_time	tx_power	tx_time	signal_power	tx_power	packet_size
2	rx_time	tx_time	rx_time	ecl	ecl	rlc_ul
3	ecl	rx_time	rlc_ul	snr	rlc_ul	rlc_dl
4	snr	ecl	mac_ul	rsrq	mac_ul	mac_ul
5	signal_power	rlc_ul	packet_size	rlc_dl	packet_size	signal_power
6	rsrq	mac_ul	mac_dl	rsrp	mac_dl	mac_dl
7	rlc_dl	packet_size	signal_power	mac_dl	rlc_dl	rsrp
8	rsrp	mac_dl	rlc_dl	rssi	rssi	rssi

TABLE 3. Custom combinations chosen based on previous analyses.

No.	Custom combination
1.	rx_time
2.	tx_time
3.	rx_time, tx_time
4.	rx_time, tx_time, ecl
5.	rsrp, snr, ecl

and subsequently forecast outcomes based on new predictor values, the application of regression models presents itself as an optimal methodological approach. Regression analysis enables the quantification of the influence of each predictor variable on the dependent variable, providing insights into the underlying dynamics of the system under study [47]. Through this statistical technique, we can develop a predictive model that facilitates accurate forecasting of energy consumption given novel sets of radio parameter values. An expanded and more formal description of the different well-known, proven regression models [48], [49], [50], [51] used in this study is given in the Table 4:

B. METRICS

Four metrics were utilized for evaluating the results obtained in this study. We use three standard metrics for regression analysis and one "non-standard" – *Accuracy*. Accuracy is used not only to obtain information about the model's correctness but also to determine whether the model is overestimating or underestimating energy consumption. This provides an insight into its "conservativeness" in terms of prediction. Definitions of these metrics are given as follows:

- **Accuracy** – measures the average ratio of predicted values to the actual values, defined as presented in 1.

$$Accuracy = \frac{1}{n}\sum_{i=1}^{n}\frac{\hat{y}_i}{y_i} \tag{1}$$

- **MAE (Mean Absolute Error)** – the average of the absolute differences between the original and predicted values, indicating how close the predictions are to the actual values. Formula for MAE calculation is displayed in 2.

$$MAE = \frac{1}{n}\sum_{i=1}^{n}|\hat{y}_i - y_i| \tag{2}$$

- **MSE (Mean Squared Error)** – the average of the squared differences between the original and predicted values, highlighting larger errors more than smaller ones. The definition of MSE is depicted in 3.

$$MSE = \frac{1}{n}\sum_{i=1}^{n}(\hat{y}_i - y_i)^2 \tag{3}$$

- **R-squared (Coefficient of Determination)** – indicates how well the predicted values fit the actual values, ranging from 0 to 1. A higher value means a better fit, with 1 representing a perfect fit. This coefficient is calculated as shown in 4.

$$R^2 = 1 - \frac{\sum_{i=1}^{n}(y_i - \hat{y}_i)^2}{\sum_{i=1}^{n}(y_i - \bar{y})^2} \tag{4}$$

VIII. EXPERIMENTAL RESULTS AND ANALYSIS

The following subsections provide a detailed analysis of the experimental results. In the subsection VIII-A, we present a general comparison of the selected models and their respective performances. The subsection VIII-B discusses the memory consumption of the models used in the study, comparing two different feature sets: one that includes all available features, and another that includes only a single temporal parameter, RX time. In the subsection VIII-C, we provide a comprehensive overview of the model's performance in predicting modem energy consumption based on various feature sets. Finally, we provide a comparison of our solution with other similar approaches found in the literature.

A. ANALYSIS OF MODELS

The models, as presented in Tables 5, 6, 7, and 8, can be classified into two categories based on performance and memory consumption (outlined in Table 9). Those are: *excellent* and *decent*. The *excellent* group, determined according to these criteria, includes DTR, GBR, XGBR,

TABLE 4. Summary of regression models and their main characteristics.

Abbr.	Type	Main Characteristic	Strengths	Weaknesses
		Regression Model		
DTR	Tree-based	*Decision Trees* Simple, interpretable rules	Handles non-linear data well	Prone to overfitting
ERT	Tree-based ensemble	*Extremely Randomized Trees* Randomized splits	Reduces overfitting risk	Less interpretable
LAR	Linear (Regularized)	*Lasso* L1 regularization	Feature selection, reduces overfitting	Can underfit with strong L1, requires careful tuning of regularization parameter
LIR	Linear	*Linear* Fits linear relationships	Simple and interpretable, computationally efficient	Assumes linear relationships
RFR	Tree-based ensemble	*Random Forest* Combines predictions from multiple trees, bagging	Robust and accurate	Less interpretable, requires careful tuning
XGBR	Gradient Boosting	*XGBoost* Boosted trees with regularization	High performance, fast and scalable	Complexity, requires careful tuning
GBR	Gradient Boosting	*Gradient Boosting* Iterative learning, loss minimization	Excellent for structured data	Prone to overfitting
KNR	Instance-based	*K-neighbors* Predictions based on neighbors	Simple, non-parametric	Sensitive to noise and scaling
RR	Linear (Regularized)	*Ridge* L2 regularization	Reduces overfitting, handles well highly correlated features	Sensitive to the choice of the regularization parameter
ENR	Linear (Regularized)	*Elastic Net* Combination of L1 and L2 regularization	Balances feature selection and shrinkage	Requires parameter tuning
PR	Polynomial Extension	*Polynomial* Fits polynomial relationships	Captures non-linear patterns	Prone to overfitting

and PR. For the DTR and GBR models, depths were adjusted between 2 and 20, and 10 and 25, respectively. Results indicate that optimal performance metrics and memory efficiency were achieved with a depth of 3 for DTR and 25 for GBR. XGBR yielded the highest performance across all metrics, with consistent memory usage, establishing it as the best-performing model. Lastly, PR outperformed LR with modestly higher memory consumption, which was deemed acceptable and thus supports its classification within the *excellent* group.

The second group encompasses a diverse set of models, including ENR, ERT, KNR, LAR, LIR, RFR, and RR. LAR and its derivative, ENR, show strong performance when transmission and reception times are part of the feature set. However, performance declines significantly in their absence. ERT and RFR models deliver high performance across all evaluated metrics, though this comes at the cost of substantial memory requirements. In this experiment, the number of estimators for these regressors was varied between 5 and 500, with an optimal value observed at 5. Thus, ERT and RFR are recommended primarily for applications requiring high performance in environments without memory limitations. KNR is included in this group due to its slightly higher memory consumption compared to GBR, though it achieves similar performance. Notably, KNR's memory footprint remains constant regardless of the number of neighbors specified. Finally, the LIR and RR models achieve stable, moderate results, with performance unaffected by the presence or absence of transmission and reception times in the feature set, though both remain outperformed by models in the *excellent* group.

To conclude, processed models can be categorized into two groups based on their performance and memory consumption:

- *Excellent* – DTR, GBR, XGBR and PR;
- *Decent* – ENR, ERT, KNR, LAR, LIR, RFR and RR;

B. MEMORY FOOTPRINT OF MODELS

As presented in the second column of Table 9, the memory footprint for the feature set that includes all features shown in Fig. 8 varies depending on the models used. The smallest footprint is observed in the DTR, ENR, LAR, LIR, PR, and RR, all of which use less than 3kB of memory. On the other hand, largest memory consumption is observed in the ERT, RFR, and KNR. Despite their high memory consumption,

TABLE 5. Performance of models with extensive feature sets.

Metric	Combination	DTR	GBR	PR	XGBR	ENR	ERT	KNR	LAR	LIR	RFR	RR
Acc	ALL	1.050	1.087	1.049	1.034	1.099	**1.023**	**1.022**	1.103	1.069	**1.024**	1.069
	NT	1.229	1.240	1.140	1.172	1.428	1.115	1.106	1.476	1.164	1.105	1.164
	RNT	1.229	1.244	1.154	1.181	1.428	1.127	1.112	1.476	1.193	1.128	1.193
MAE	ALL	0.044	0.044	0.055	0.033	0.062	**0.025**	**0.029**	0.062	0.062	**0.025**	0.062
	NT	0.118	0.118	0.099	0.096	0.196	0.077	0.077	0.210	0.107	0.077	0.107
	RNT	0.118	0.118	0.103	0.099	0.196	0.085	0.085	0.210	0.114	0.088	0.114
MSE	ALL	0.0022	0.0019	0.0026	**0.0015**	0.0037	0.0019	**0.0015**	0.0037	0.0029	**0.0015**	0.0029
	NT	0.0096	0.0085	0.0059	0.0063	0.0155	0.0056	0.0070	0.0171	0.0074	0.0056	0.0074
	RNT	0.0096	0.0089	0.0067	0.0067	0.0155	0.0056	0.0067	0.0171	0.0085	0.0059	0.0085
R2	ALL	0.903	0.913	0.887	0.931	0.846	**0.932**	**0.936**	0.845	0.864	**0.938**	0.864
	NT	0.576	0.622	0.728	0.714	0.313	0.760	0.693	0.256	0.672	0.756	0.672
	RNT	0.576	0.612	0.697	0.709	0.311	0.770	0.703	0.256	0.625	0.729	0.625

TABLE 6. Performance of models with K-best generated feature sets.

Metric	Combination	DTR	GBR	XGBR	PR	ENR	ERT	KNR	LAR	LIR	RFR	RR
Acc	$\mathbf{FR}_4$	1.050	1.084	1.064	1.035	1.099	**1.027**	**1.025**	1.102	1.093	**1.023**	1.093
	$\mathbf{FR}_8^{NT}$	1.229	1.246	1.153	1.181	1.428	1.112	1.086	1.476	1.177	1.122	1.177
	$\mathbf{FR}_6^{NT}$	1.233	1.251	1.219	1.197	1.428	1.177	1.160	1.476	1.233	1.177	1.233
	$\mathbf{FR}_4^{NT}$	1.233	1.248	1.218	1.206	1.428	1.188	1.275	1.476	1.233	1.193	1.234
MAE	$\mathbf{FR}_4$	0.044	0.044	0.055	**0.033**	0.062	**0.033**	**0.033**	0.062	0.0629	**0.033**	0.062
	$\mathbf{FR}_8^{NT}$	0.118	0.118	0.103	0.099	0.196	0.085	0.088	0.210	0.111	0.085	0.111
	$\mathbf{FR}_6^{NT}$	0.118	0.122	0.118	0.107	0.196	0.099	0.122	0.210	0.122	0.099	0.122
	$\mathbf{FR}_4^{NT}$	0.118	0.122	0.111	0.111	0.196	0.107	0.144	0.210	0.122	0.111	0.122
MSE	$\mathbf{FR}_4$	0.0019	0.0019	0.0026	**0.0015**	0.0033	**0.0015**	**0.0015**	0.0033	0.0033	**0.0015**	0.0033
	$\mathbf{FR}_8^{NT}$	0.0096	0.0085	0.0063	0.0067	0.0155	0.0056	0.0070	0.0171	0.0078	0.0056	0.0078
	$\mathbf{FR}_6^{NT}$	0.0096	0.0089	0.0096	0.0077	0.0155	0.0077	0.0115	0.0171	0.0100	0.0074	0.0100
	$\mathbf{FR}_4^{NT}$	0.0096	0.0089	0.0092	0.0085	0.0155	0.0096	0.0148	0.0171	0.0100	0.0089	0.0100
R2	$\mathbf{FR}_4$	0.903	0.913	0.878	**0.923**	0.845	**0.928**	**0.924**	0.844	0.849	0.921	0.849
	$\mathbf{FR}_8^{NT}$	0.576	0.615	0.711	0.698	0.313	0.770	0.687	0.256	0.653	0.748	0.653
	$\mathbf{FR}_6^{NT}$	0.570	0.606	0.579	0.652	0.313	0.685	0.500	0.256	0.563	0.662	0.563
	$\mathbf{FR}_4^{NT}$	0.570	0.603	0.582	0.630	0.311	0.599	0.352	0.256	0.564	0.601	0.564

TABLE 7. Performance of models with heatmap generated feature sets.

Metric	Combination	DTR	GBR	XGBR	PR	ENR	ERT	KNR	LAR	LIR	RFR	RR
Acc	TX	1.071	1.105	1.086	1.054	1.148	**1.029**	**1.032**	1.151	1.126	**1.032**	1.126
	RX	1.063	1.094	1.063	1.047	1.178	1.038	1.035	1.185	1.141	1.037	1.141
	CE mode	1.248	1.246	1.235	1.179	1.560	1.091	1.087	1.576	1.243	1.103	1.244
MAE	TX	0.051	0.055	0.062	0.044	0.085	**0.033**	**0.033**	0.085	0.077	**0.029**	0.077
	RX	0.048	0.048	0.070	0.040	0.099	0.037	0.040	0.099	0.092	0.037	0.092
	CE mode	0.118	0.118	0.118	0.099	0.251	0.077	0.077	0.259	0.122	0.085	0.122
MSE	TX	0.0029	0.0026	0.0033	0.0022	0.0044	0.0022	0.0026	0.0044	0.0041	**0.0019**	0.0041
	RX	0.0026	0.0022	0.0033	**0.0019**	0.0070	**0.0019**	0.0026	0.0074	0.0063	0.0022	0.0063
	K3	0.0099	0.0085	0.0096	0.0070	0.0215	0.0059	0.0070	0.0229	0.0099	0.0067	0.0099
R2	TX	0.860	0.874	0.849	0.895	0.797	**0.920**	0.886	0.796	0.814	0.908	0.814
	RX	0.879	0.894	0.852	**0.909**	0.682	**0.914**	0.885	0.672	0.722	0.889	0.722
	CE mode	0.558	0.618	0.575	0.682	0.052	0.750	0.683	0.078	0.551	0.708	0.551

TABLE 8. Performance of models with custom feature sets.

Metric	Combination	DTR	GBR	XGBR	PR	ENR	ERT	KNR	LAR	LIR	RFR	RR
Acc	TX	1.071	1.105	1.097	1.062	1.148	1.057	1.058	1.151	1.145	1.054	1.145
	RX	1.073	1.108	1.088	1.071	1.184	1.067	1.075	1.187	1.182	1.073	1.182
	T+R	1.050	1.084	1.065	1.041	1.099	**1.030**	**1.025**	1.102	1.096	**1.024**	1.096
	T+E	1.068	1.103	1.077	1.062	1.184	1.058	1.066	1.187	1.132	1.066	1.132
	RSSI	1.508	1.503	1.565	1.480	1.573	1.464	1.504	1.576	1.560	1.459	1.560
MAE	TX	0.051	0.055	0.062	0.048	0.085	0.044	0.044	0.085	0.081	0.044	0.081
	RX	0.055	0.055	0.077	0.051	0.099	0.062	0.062	0.103	0.099	0.062	0.099
	T+R	0.044	0.044	0.059	0.037	0.062	**0.033**	**0.029**	0.062	0.062	**0.033**	0.062
	T+E	0.051	0.055	0.070	0.051	0.099	0.059	0.059	0.103	0.088	0.055	0.088
	RSSI	0.233	0.229	0.255	0.225	0.255	0.222	0.244	0.259	0.255	0.222	0.255
MSE	TX	0.0029	0.0029	0.003	0.0029	0.0044	0.0033	0.0029	0.0044	0.0044	0.0029	0.0044
	RX	0.0025	0.0025	0.0037	0.0022	0.0074	0.0040	0.0037	0.0074	0.0074	0.0037	0.0074
	T+R	0.0018	0.0018	0.0025	0.0018	0.0033	**0.0014**	**0.0014**	0.0033	0.0033	**0.0014**	0.0033
	T+E	0.0025	0.0022	0.0033	0.0022	0.0074	0.0033	0.0033	0.0074	0.0059	0.0029	0.0059
	RSSI	0.0207	0.0199	0.0225	0.0199	0.0225	0.0207	0.0303	0.0229	0.0225	0.0207	0.0225
R2	TX	0.861	0.866	0.828	0.870	0.797	0.853	0.862	0.796	0.798	0.859	0.798
	RX	0.880	0.881	0.833	0.888	0.668	0.820	0.833	0.668	0.668	0.838	0.668
	T+R	0.903	0.913	0.875	0.911	0.845	**0.927**	**0.931**	0.844	0.846	**0.925**	0.846
	T+E	0.879	0.887	0.845	0.893	0.668	0.849	0.840	0.668	0.734	0.857	0.734
	RSSI	0.090	0.127	0.019	0.121	0.005	0.096	-0.323	-0.001	0.019	0.097	0.019

these models, particularly ERT and RFR, deliver some of the best results in terms of overall model performance. The middle tier of models includes the GBR and XGBR, where the XGBR demonstrates a slightly better and more consistent memory efficiency, particularly when smaller feature sets are used.

The third column of Table 9 presents the size of the memory footprint for a feature set consisting of only one parameter. To generate this memory footprint, RX time, the feature that produces the best results among single feature sets, was used. However, it should be noted that the results are very similar when different single feature sets are used. As observed from the comparison between the second and third columns, the difference in memory footprint across all models is generally negligible, but in some cases, it is worth considering. For DTR, the difference is minimal when a smaller tree depth is used. However, as the depth increases, the difference becomes more pronounced. In this context, DTRs still provide sufficiently good results with a small depth, making the increase in memory footprint less impactful.

For ENR, LAR, LIR, PR, and RR, there is a slight improvement in memory consumption, but it is not significantly better. Additionally, GBR and XGBR are again somehow special. As mentioned earlier, these models, especially the XGBR, exhibit a fairly consistent memory consumption pattern, which has been slightly, but negligibly, improved with the reduction in feature set size.

On the other hand, the reduction in feature set size had a substantial impact on the memory footprint of ERT, RFR, and KNR. In these cases, memory consumption dropped by approximately 50%. When using certain features, such as RX time in this case, which can deliver acceptable overall performance on their own, this becomes particularly interesting since good performance can be achieved with a significant reduction in memory consumption. However, it should be noted that similar performance could be achieved using much smaller models.

Memory footprint analysis provides several conclusions:

- Models can be categorized into three groups based on their memory footprint:
  - -- *Smallest* – DTR, ENR, LAR, LIR, PR and RR;
  - -- *Mid-sized* – GBR and XGBR;
  - -- *Largest* – ERT, RFR and KNR;
- Variance in a number of input features does not significantly reduce model memory footprint in most cases. The most significant reduction is achieved by ERT, RFR and KNR.

C. PERFORMANCE OF FEATURE SETS

The quality of energy consumption predictions based on the discussed models, concerning various input feature sets, is detailed in Tables 5, 6, 7, and 8. Performance is assessed using four distinct metrics, which provide diverse insights. In addition to the standard MAE, MSE, and R2 metrics, accuracy is evaluated according to the definition in Section VII-B, yielding noteworthy results. In each table, the three highest results per metric are emphasized in bold. As shown in the aforementioned tables, this accuracy metric consistently exceeds 1.0. This finding indicates that, on average, the regressors predict energy consumption values higher than the actual values. This outcome is significant as it suggests that models will tend to overestimate energy consumption, leading to a more conservative assessment of battery lifespan.

TABLE 9. Memory footprint analysis of feature set that includes all features and feature set that includes only one input parameter.

Model	MF [kB]	MF–RX time [kB]
DTR	2.64	2.46
GBR	53.26	52.33
PR	3.18	1.17
XGBR	113.09	111.62
ENR	1.19	0.93
ERT	3310.40	1402.65
KNR	1168.00	160.53
LAR	1.19	0.92
LIR	1.22	0.84
RFR	2094.98	1087.65
RR	1.09	0.82

TABLE 10. Extensive parameter sets.

Set name	Parameters
T	packet_size, signal_power, tx_power, tx_time, snr, rlc_ul, rlc_dl, mac_ul
R	packet_size, signal_power, tx_power, rx_time, rsrq, rlc_ul, mac_dl, mac_ul
E	packet_size, rlc_ul, mac_ul, tx_power, rssi, rsrq, ecl, rlc_dl

Table 5 presents the results of testing various feature sets, encompassing nearly all parameters as displayed in Table 10. The first set (ALL) includes all parameters and demonstrates the best performance. The second set (NT) is similar to set ALL but omits time-related parameters (tx_time and rx_time). The third set (RNT) aims to retain as many parameters from set NT as possible while minimizing performance degradation. The removal of temporal parameters leads to reduced performance in both sets NT and RNT compared to set ALL. Nonetheless, these sets still perform well, as their R2 scores surpass the 0.7 threshold for some models. Consequently, Table 5, indicates that temporal parameters are critical for accurate energy consumption predictions. Their absence significantly impairs performance, even when other parameters are included.

As detailed in Section VI-A, we can group parameters by the information they provide listed in Table 1, leading to 36 distinct combinations of parameter sets. Given the

extensive number of possible combinations, this study focuses on three selected feature sets, each representing the best-performing set containing members of Group 3 from Table 1. Although Table 5 demonstrates that temporal parameters are foundational for the most effective feature sets, our goal is to identify the optimal combination of features based on the feature correlation heatmap. The combinations are detailed in Table 11. The final combination in this table omits temporal parameters, relying instead on the CE mode. The first two combinations, which include temporal parameters, yield results only slightly inferior to the set ALL from Table 5. This suggests that incorporating a single temporal parameter along with additional radio channel quality parameters can still produce significant results. In contrast, the third feature set, while showing similar performance to sets NT and RNT, offers a reduction in the number of input features.

Additionally, removing independent parameter inputs, as described in VI-A, results in an average decrease in accuracy between 1-3%. This suggests that these parameters are not essential for predicting energy consumption, but still, there is a benefit of using those additional parameters for enhancing model performance. Therefore, the performance of models that do not utilize independent parameters as inputs is not presented.

TABLE 11. Feature correlation heatmap parameter sets.

Set name	Parameters
ALL	packet_size, signal_power, tx_power, tx_time, rx_time, ecl, snr, rsrq, rlc_ul, rlc_dl, mac_ul, mac_dl, rsrp, rssi
NT	packet_size, signal_power, tx_power, ecl, snr, rsrq, rlc_ul, rlc_dl, mac_ul, mac_dl, rsrp, rssi
RNT	signal_power, ecl, snr, rsrq, rlc_ul, rlc_dl, mac_ul, mac_dl, rssi

Table 6 provides performance results for model input feature sets determined by the K-Best feature extractor. As shown in Table 5, combinations with temporal parameters provide better results, we limited the Table 6 to a single combination with temporal parameter, which provides the best result of all K-Best regressions. This combination was generated by F-regression and utilizes only 4 parameters. The list of parameters generated by K-Best regressions is given in Table 2. To provide a consistent comparison, Table 6 provides additional three combinations that do not contain temporal parameters generated utilizing F-regression for 4, 6, and 8 parameters. The table confirms the conclusion that sets containing a temporal parameter provide significantly better results, but it also shows that combinations without them can give good enough results as shown with a combination with 8 parameters. Nevertheless, the reduction of some parameters in sets that do not contain temporal parameter leads to a decrease in performance with each dropped parameter.

Table 8 provides an overview of the results for custom input feature sets, which were created empirically with the idea of achieving high performance while using the absolute lowest possible number of input parameters. Following up on the conclusions made about sets that contain temporal parameters, we created custom sets given in Table 13. The first two sets are single-element sets that contain distinct temporal parameter. Interestingly, a single temporal parameter is enough to produce better performance than all non-temporal parameters combined. This further confirms the importance of temporal parameters in the prediction of energy consumption of NB-IoT modems. The third set combines two temporal parameters and generates even better results. The fourth set is created by adding the CE mode parameter to the third set, as those three elements provide the best correlation to energy consumption, as calculated by feature correlation heatmap and presented in Fig. 8. Nevertheless, the fourth set produces better results than the first two, but worse than the third set. We attribute this behavior to the binary value of the CE mode. At last, the fifth set contains the RSSI parameter as representative of all single-element non-temporal parameter sets which were not able to predict energy consumption with any degree of certainty.

Finally, a comparison of the energy consumption predictions made by the best-scoring model – RFR, which was trained using the dataset containing parameters from set ALL is depicted in Fig. 9. The x-axis represents actual, measured energy consumption samples collected from onboard current measurements. On the other hand, the y-axis represents the energy consumption values predicted utilizing the RFR model, which demonstrated the highest accuracy among all regression models, achieving R2 value of 93.8%.

Fig. 9 displays 1176 data points from the test set, the majority of which are clustered near the main diagonal. This positioning indicates a high level of accuracy in the model's energy consumption predictions.

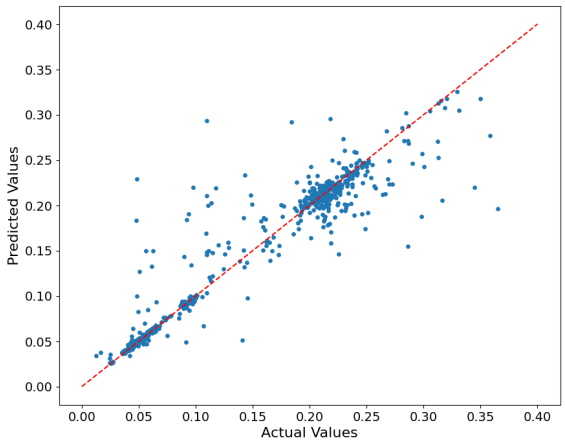

FIGURE 9. Comparison of energy consumption predicted utilizing RFR and actual energy consumption.

TABLE 12. Comparisons with the other approaches.

Parameters	Paper				
	[30]	[29]	[20]	[19]	**OUR**
Approach	ML	ML	Analytical	Analytical	ML
Network technology	IEEE 802.15.4	GSM	NB-IoT/LTE-M	NB-IoT	NB-IoT
Current Measurement	–	external	external	external	on-board
Network module	–	SIM800L	EVK-N211/-R410M	Quectel BG96	Quectel BC68
Dataset	existing	custom	–	–	custom
Best-scoring model	Deep NN	RF	–	–	RF
Accuracy	up to 98%	up to 98%	[95-100]%	[84.62-99.66]%	93.8%

ML - **M**achine **L**earning, **NN** - **N**eural **N**etwork, **RF** - **R**andom **F**orest

TABLE 13. Custom parameter sets.

Set name	Parameters
C1	tx_time
C2	rx_time
C3	tx_time, rx_time
C4	tx_time, rx_time, ecl
C5	rssi

To sum up, analysis of the performance of presented models gives the following conclusions:

- accuracy metric consistently exceeds value 1.0, indicating that models tend to overestimate energy consumption, leading to a more conservative assessment of battery lifespan;
- the best-set performance-wise is set ALL, which contains all available features and achieves 93.8% R2 metric value for RFR;
- enhancing a single temporal parameter with additional radio channel quality parameters produces significant improvements;
- the removal of temporal parameters leads to reduced performance;
- to overcome the absence of temporal parameters, models require a combination of all non-correlated features to produce results that exceed 70% R2 metric threshold;
- a single temporal parameter is enough to produce better performance than all non-temporal parameters combined;
- single non-temporal parameter sets are not able to predict energy consumption with any degree of certainty.

D. COMPARISON WITH OTHER APPROACHES

Table 12 provides a comparison of key attributes across several related works in this field. Some main observations are as follows.

As can be seen from the table, the studies presented in related papers differ in approaches. Some of them utilize ML techniques in energy consumption estimation, while, on the other hand, some of them use a strictly analytical approach.

In terms of network technology used in the studies, the papers that utilize ML techniques analyze different network standards from our study. Specifically, [30] employs IEEE 802.15.4, a protocol widely used in low-power wireless personal area networks, while [29] uses GSM. On the other hand, both papers that adopt an analytical approach, [19] and [20], use NB-IoT in their experimental study, which aligns them more with our study.

Also, all the other studies rely on external current measurement devices, while our study utilizes an onboard measurement technique, which enables us to isolate the consumption of the NB-IoT module from the rest of the on-board circuitry.

The accuracy comparison reflects that our solution presents competitive results, and in some cases, even better than other similar approaches. However, it's worth mentioning that these studies are based on specific network modules and technologies. Therefore, the comparison between those devices cannot be generalized to a conclusion that our methodology is better or worse, as the energy footprint of a device is implementation-specific.

IX. CONCLUSION

Accurately estimating energy consumption in edge devices is a critical challenge due to the non-linear discharge characteristics of batteries, which complicate the interpretation of output voltage measurements. Addressing this challenge requires robust methods for estimating energy consumption to enable precise predictions of device operational lifespan.

In this paper, we propose a methodology and conduct a comprehensive analysis of energy consumption estimation for a custom-fabricated device equipped with an NB-IoT module and on-board current measuring capabilities, employing various ML algorithms. We constructed a custom dataset comprising 5,880 data points, with each data point encapsulating information about corresponding radio and temporal parameters, and actual current consumption.

Next, we presented a detailed input feature analysis to investigate the mutual correlations among parameters and established a feature selection process to identify those most suitable for energy consumption estimation. Subsequently,

different regression models were analyzed to assess their suitability for this specific task.

In the results, we showed that:

- temporal parameters can be used solely to estimate energy consumption with great certainty;
- all models overestimate which is a good sign, because of its conservative approach in terms of battery change;
- individual performance of the radio channel quality parameters is suboptimal. However, their combination yields significantly enhanced outcomes.

As for the regression models, we divided all analyzed models into two groups: excellent and good. The excellent group, which consists of DTRs, GBR, XGBR, and PR, showed the best results among all metrics. Among them, DTRs achieved the smallest memory footprint with good estimation performance, while XGBR showed small memory model variability with great performance in terms of estimation. Good models comprise ENR, ERT, KNR, LAR, LIR, RFR, and RR. Some of them, such as ERT and RFR, performed excellently but had large memory footprints. With RFR using all available parameters, we achieved the best result of 93.8% R2 value. Finally, regressors such as LAR, RR, and their derivative, ENR, showed good results with temporal features but poor results when using other input combinations.

A. FUTURE WORK

For future work, the following things should be considered:

- test more sophisticated ML models in order to achieve better performance in terms of energy consumption estimation;
- experiment with additional feature selection methods to deepen the understanding of the correlation between parameters and consumption;
- update the existing dataset with a wider range of data points that reflect poorer radio conditions than the current ones;
- integrate ML models to achieve on-the-edge self-estimation of energy consumption by running inference on the device;
- testing of battery lifetime prediction based on proposed models;
- generating a more extensive dataset, especially when it comes to the variance in CE mode (including CE2), and TX power levels.

X. DATASET

The dataset used in this study is available at: https://github.com/VladimirNikic/nbiot_energy_consumption_dataset.git accessed on 25 November 2024.

REFERENCES

[1] IoT Analytics. (2024). *State of IoT 2024: Number of Connected Iot Devices Growing 13% To 18.8 Billion Globally*. Accessed: Nov. 11, 2024. [Online]. Available: https://iot-analytics.com/number-connected-iot-devices/

[2] Marketing Team. (2019). *Advantages and Special Features of Lithium Thionyl Chloride Batteries*. Jauch Blog. Accessed: Dec. 21, 2024. [Online]. Available: https://www.jauch.com/blog/en/advantages-and-special-features-of-lithium-thionyl-chloride-batteries/

[3] E. Dahlman, S. Parkvall, and J. Skold, *4G: LTE/LTE-Advanced for Mobile Broadband*. New York, NY, USA: Academic, 2013.

[4] Y. Abadade, A. Temouden, H. Bamoumen, N. Benamar, Y. Chtouki, and A. S. Hafid, "A comprehensive survey on TinyML," *IEEE Access*, vol. 11, pp. 96892–96922, 2023.

[5] N. Schizas, A. Karras, C. Karras, and S. Sioutas, "TinyML for ultra-low power AI and large scale IoT deployments: A systematic review," *Future Internet*, vol. 14, no. 12, p. 363, Dec. 2022.

[6] R. K. Singh, P. P. Puluckul, R. Berkvens, and M. Weyn, "Energy consumption analysis of LPWAN technologies and lifetime estimation for IoT application," *Sensors*, vol. 20, no. 17, p. 4794, Aug. 2020. [Online]. Available: https://www.mdpi.com/1424-8220/20/17/4794

[7] S. Duhovnikov, A. Baltaci, D. Gera, and D. A. Schupke, "Power consumption analysis of NB-IoT technology for low-power aircraft applications," in *Proc. IEEE 5th World Forum Internet Things (WF-IoT)*, Apr. 2019, pp. 719–723.

[8] P. Jörke, R. Falkenberg, and C. Wietfeld, "Power consumption analysis of NB-IoT and eMTC in challenging smart city environments," in *Proc. IEEE Globecom Workshops (GC Wkshps)*, Dec. 2018, pp. 1–6.

[9] S. Popli, R. K. Jha, and S. Jain, "A survey on energy efficient narrowband Internet of Things (NBIoT): Architecture, application and challenges," *IEEE Access*, vol. 7, pp. 16739–16776, 2019.

[10] M. T. Abbas, K.-J. Grinnemo, J. Eklund, S. Alfredsson, M. Rajiullah, A. Brunstrom, G. Caso, K. Kousias, and Ö. Alay, "Energy-saving solutions for cellular Internet of Things–A survey," *IEEE Access*, vol. 10, pp. 62073–62096, 2022.

[11] D. Yang, X. Huang, J. Huang, X. Chang, G. Xing, and Y. Yang, "A first look at energy consumption of NB-IoT in the wild: Tools and large-scale measurement," *IEEE/ACM Trans. Netw.*, vol. 29, no. 6, pp. 2616–2631, Dec. 2021.

[12] M. Lukic, S. Sobot, I. Mezei, D. Vukobratovic, and D. Danilovic, "In-depth real-world evaluation of NB-IoT module energy consumption," in *Proc. IEEE Int. Conf. Smart Internet Things (SmartIoT)*, Aug. 2020, pp. 261–265.

[13] J. Lee and J. Lee, "Prediction-based energy saving mechanism in 3GPP NB-IoT networks," *Sensors*, vol. 17, no. 9, p. 2008, Sep. 2017.

[14] G. Tsoukaneri, F. D. García, and M. K. Marina, "Narrowband IoT device energy consumption characterization and optimizations," in *Proc. Int. Conf. Embedded Wireless Syst. Netw.* Junction Publishing, Feb. 2020, pp. 1–12.

[15] S. A. Manzar, S. Verma, and S. H. Gupta, "Analysis and optimization of downlink energy in NB-IoT," *Sustain. Comput., Informat. Syst.*, vol. 35, Sep. 2022, Art. no. 100757.

[16] M. Lauridsen, R. Krigslund, M. Rohr, and G. Madueno, "An empirical NB-IoT power consumption model for battery lifetime estimation," in *Proc. IEEE 87th Veh. Technol. Conf. (VTC Spring)*, Jun. 2018, pp. 1–5.

[17] P. Andres-Maldonado, M. Lauridsen, P. Ameigeiras, and J. M. Lopez-Soler, "Analytical modeling and experimental validation of NB-IoT device energy consumption," *IEEE Internet Things J.*, vol. 6, no. 3, pp. 5691–5701, Jun. 2019.

[18] F. Michelinakis, A. S. Al-Selwi, M. Capuzzo, A. Zanella, K. Mahmood, and A. Elmokashfi, "Dissecting energy consumption of NB-IoT devices empirically," *IEEE Internet Things J.*, vol. 8, no. 2, pp. 1224–1242, Jan. 2021.

[19] S. M. Z. Khan, M. M. Alam, Y. Le Moullec, A. Kuusik, S. Pärand, and C. Verikoukis, "An empirical modeling for the baseline energy consumption of an NB-IoT radio transceiver," *IEEE Internet Things J.*, vol. 8, no. 19, pp. 14756–14772, Oct. 2021.

[20] A. Sørensen, H. Wang, M. J. Remy, N. Kjettrup, R. B. Sørensen, J. J. Nielsen, P. Popovski, and G. C. Madueño, "Modeling and experimental validation for battery lifetime estimation in NB-IoT and LTE-M," *IEEE Internet Things J.*, vol. 9, no. 12, pp. 9804–9819, Jun. 2022.

[21] J. P. GarcaMartn and A. Torralba, "Energy consumption analytical modeling of NB-IoT devices for diverse IoT applications," *Comput. Netw.*, vol. 232, Aug. 2023, Art. no. 109855. [Online]. Available: https://www.sciencedirect.com/science/article/pii/S1389128623003006

[22] R. Burczyk, A. Czapiewska, M. Gajewska, and S. Gajewski, "LTE and NB-IoT performance estimation based on indicators measured by the radio module," *Electronics*, vol. 11, no. 18, p. 2892, Sep. 2022.

[23] W. Law, S. Li, and K. M. G. Chavez, "Empirical comparison of the energy consumption of cellular Internet of Things technologies," *IEEE Access*, vol. 11, pp. 106374–106386, 2023.
[24] *Cellular System Support for Ultra-low Complexity and Low Throughput Internet of Things (CIoT)*, Standard TR 145 050-V13.1.0, 3GPP, 2015. [Online]. Available: https://www.3gpp.org/dynareport/45820.htm
[25] N. Labdaoui, F. Nouvel, and S. Dutertre, "NB-IoT power consumption: A comparison of SFR and objenious network operators," in *Proc. 17ème Colloque du GDR SoC2*, Jun. 2023, pp. 1–3.
[26] S. K. Kalyankar, G. D. González, Y. Liang, and Y. L. Guan, "An approach to enhance NB-IoT device life," in *Proc. IEEE INC-USNC-URSI Radio Sci. Meeting (Joint AP-S Symp.)*, Jul. 2024, pp. 174–175.
[27] Z. Hu, G. Xue, Y. Chen, M. Li, M. Wang, and F. Lv, "City-wide NB-IoT network monitoring and diagnosing," *Wireless Commun. Mobile Comput.*, vol. 2022, no. 1, Apr. 2022, Art. no. 3153274.
[28] M. Nurgaliyev, A. Saymbetov, Y. Yashchyshyn, N. Kuttybay, and D. Tukymbekov, "Prediction of energy consumption for LoRa based wireless sensors network," *Wireless Netw.*, vol. 26, no. 5, pp. 3507–3520, Jul. 2020.
[29] V. N. Katambire, R. Musabe, A. Uwitonze, and D. Mukanyiligira, "Battery-powered RSU running time monitoring and prediction using ML model based on received signal strength and data transmission frequency in V2I applications," *Sensors*, vol. 23, no. 7, p. 3536, Mar. 2023.
[30] M. Ateeq, F. Ishmanov, M. K. Afzal, and M. Naeem, "Multi-parametric analysis of reliability and energy consumption in IoT: A deep learning approach," *Sensors*, vol. 19, no. 2, p. 309, Jan. 2019.
[31] L. D. Rodić, T. Županović, T. Perković, P. Šolić, and J. J. Rodrigues, "Machine learning and soil humidity sensing: Signal strength approach," *ACM Trans. Internet Technol. (TOIT)*, vol. 22, no. 2, pp. 1–21, 2021.
[32] R. Falkenberg, B. Sliwa, N. Piatkowski, and C. Wietfeld, "Machine learning based uplink transmission power prediction for LTE and upcoming 5G networks using passive downlink indicators," in *Proc. IEEE 88th Veh. Technol. Conf. (VTC-Fall)*, Aug. 2018, pp. 1–7.
[33] H. A. H. Alobaidy, M. J. Singh, R. Nordin, N. F. Abdullah, C. G. Wei, and M. L. S. Soon, "Real-world evaluation of power consumption and performance of NB-IoT in Malaysia," *IEEE Internet Things J.*, vol. 9, no. 13, pp. 11614–11632, Jul. 2022.
[34] M. Martí-Florences, A. Cecilia, and R. Costa-Castelló, "Modelling and estimation in lithium-ion batteries: A literature review," *Energies*, vol. 16, no. 19, p. 6846, Sep. 2023.
[35] P. Chen, Z. Mao, C. Lu, B. Li, W. Ding, and J. Li, "Effective capacity early estimation of lithium thionyl chloride batteries for autonomous underwater vehicles," *J. Power Sources*, vol. 595, Mar. 2024, Art. no. 234046.
[36] A. G. Olabi, A. A. Abdelghafar, B. Soudan, A. H. Alami, C. Semeraro, M. Al Radi, M. Al-Murisi, and M. A. Abdelkareem, "Artificial neural network driven prognosis and estimation of lithium-ion battery states: Current insights and future perspectives," *Ain Shams Eng. J.*, vol. 15, no. 2, Feb. 2024, Art. no. 102429.
[37] S. Shen, M. Sadoughi, X. Chen, M. Hong, and C. Hu, "A deep learning method for online capacity estimation of lithium-ion batteries," *J. Energy Storage*, vol. 25, Oct. 2019, Art. no. 100817.
[38] M. Lukic, S. Sobot, I. Mezei, and D. Vukobratovic, "3gpp nb-iot for smart environments: Testbed experimentation and use cases," *IEICE Proc. Ser.*, vol. 64, pp. 1–4, Mar. 2021.
[39] D. Vukobratovic, M. Lukic, I. Mezei, D. Bajovic, D. Danilovic, M. Savic, Z. Bodroski, S. Skrbic, and D. Jakovetic, "Edge machine learning in 3GPP NB-IoT: Architecture, applications and demonstration," in *Proc. 30th Eur. Signal Process. Conf. (EUSIPCO)*, Aug. 2022, pp. 707–711.
[40] Quectel. (Mar. 2018). *NB-IoT Module Series BC95-G & BC68 AT Commands Manual*. Accessed: Oct. 6, 2024. [Online]. Available: https://www.quectel.com/lpwa-iot-modules/
[41] A. P. Matz, J.-A. Fernandez-Prieto, J. Cañada-Bago, and U. Birkel, "A systematic analysis of narrowband IoT quality of service," *Sensors*, vol. 20, no. 6, p. 1636, Mar. 2020.
[42] S. Khalid, T. Khalil, and S. Nasreen, "A survey of feature selection and feature extraction techniques in machine learning," in *Proc. Sci. Inf. Conf.*, Aug. 2014, pp. 372–378.
[43] J. Cai, J. Luo, S. Wang, and S. Yang, "Feature selection in machine learning: A new perspective," *Neurocomputing*, vol. 300, pp. 70–79, Jul. 2018.
[44] P. Dhal and C. Azad, "A comprehensive survey on feature selection in the various fields of machine learning," *Int. J. Speech Technol.*, vol. 52, no. 4, pp. 4543–4581, Mar. 2022.
[45] F. Pedregosa, G. Varoquaux, A. Gramfort, V. Michel, B. Thirion, O. Grisel, M. Blondel, P. Prettenhofer, R. J. Weiss, V. Dubourg, J. Vanderplas, A. Passos, D. Cournapeau, M. Brucher, M. Perrot, and É. Duchesnay, "Scikit-learn: Machine learning in Python," *J. Mach. Learn. Res.*, vol. 12, pp. 2825–2830, Jan. 2011.
[46] M. Abadias et al. (2015). *TensorFlow: Large-scale Machine Learning on Heterogeneous Systems*. Softw. available from tensorflow.org. [Online]. Available: https://www.tensorflow.org/
[47] A. O. Sykes, "An introduction to regression analysis," Coase-Sandor Work. Paper Ser. Law Economics 20, Tech. Rep., 1993. [Online]. Available: https://chicagounbound.uchicago.edu/law_and_economics/51
[48] J. A. Alzubi, A. Nayyar, and A. Kumar, "Machine learning from theory to algorithms: An overview," *J. phys., Conf. Ser.*, vol. 1142, Nov. 2018, Art. no. 012012.
[49] T. Doan and J. Kalita, "Selecting machine learning algorithms using regression models," in *Proc. IEEE Int. Conf. Data Mining Workshop (ICDMW)*, Nov. 2015, pp. 1498–1505.
[50] Y. Tai, "A survey of regression algorithms and connections with deep learning," 2021, *arXiv:2104.12647*.
[51] I. H. Sarker, "Machine learning: Algorithms, real-world applications and research directions," *Social Netw. Comput. Sci.*, vol. 2, no. 3, p. 160, May 2021.

DUSAN BORTNIK received the B.Sc. and M.Sc. degrees in electrical engineering from the Faculty of Technical Sciences, University of Novi Sad, in 2019 and 2020, respectively, where he is currently pursuing the Ph.D. degree. He is also an Embedded Software Engineer at NXP Semiconductors Austria GmbH Co & KG. He has published one book, one peer-reviewed journal article, and four conference papers. His research interests include embedded systems and embedded software design, the Internet of Things (IoT), LPWAN, and edge computing.

VLADIMIR NIKIC received the B.Sc. and M.Sc. degrees in electrical engineering from the Faculty of Technical Sciences, University of Novi Sad, Novi Sad, Serbia, in 2019 and 2020, respectively, where he is currently pursuing the Ph.D. degree. He is also an Embedded Software Engineer at ARS Embedded Systems LLC, Novi Sad. He has published one book, one peer-reviewed journal article, and four conference papers. His research interests include embedded systems and software, machine learning at the edge, the Internet of Things (IoT), and LPWAN.

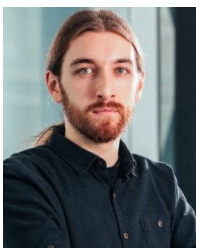

SRDJAN SOBOT received the B.Sc. and M.Sc. degrees from the University of Novi Sad (UNS), Serbia, in 2016 and 2018, respectively, where he is currently pursuing the Ph.D. degree with the Wireless Communications Laboratory, with a focus on testbeds with software-defined radio devices (SDR). His research interests include 4G/5G mobile cellular networks, cellular IoT standards, and UAV-aided networks.

DEJAN VUKOBRATOVIC (Senior Member, IEEE) received the Dr.-Ing. degree in electrical engineering from the University of Novi Sad, Serbia, in 2008. From 2009 to 2010, he was a Marie Curie Intra-European Fellow at the University of Strathclyde, Glasgow, U.K. Since 2019, he has been a Full Professor with the Department of Power, Electronics and Communication Engineering, University of Novi Sad. He has co-authored over 50 journals and 110 conference research papers mostly published in top-tier IEEE venues. His research interests include wireless communications and the Internet of Things. He was the TPC Co-Chair for IEEE VTC Spring 2020 and IEEE SmartGridComm 2022 and the General Chair for BalkanCom 2020 and IEEE CSCN 2024, while he co-authored best papers awarded at IEEE MMSP 2010 and IEEE SmartGridComm 2017.

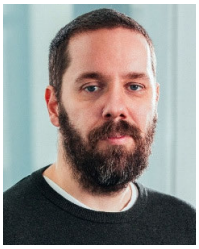

IVAN MEZEI (Senior Member, IEEE) received the Dr.-Ing. degree in electronics engineering from the University of Novi Sad, Serbia, in 2012. Since 2023, he has been a Full Professor with the DEET, FTN, University of Novi Sad. He was a principal researcher, the work package leader, a supervisor, or the team leader in several international research projects financed by the European Commission or companies. He has published two books, two book chapters, more than 15 peer-reviewed journal articles, and more than 40 conference papers. His current research interests include LPWAN Internet of Things, embedded systems, localization, wireless sensors, actuators, and robot networks. He was a reviewer of more than 20 peer-reviewed journals and more than 40 conferences, and a TPC member for more than 40 conferences.

MILAN LUKIC (Member, IEEE) received the Ph.D. degree from the Faculty of Technical Sciences, University of Novi Sad, Serbia, in 2015. He is currently an Assistant Professor with the Faculty of Technical Sciences, University of Novi Sad, Serbia. He has been involved in numerous research projects covering topics of low-power embedded systems, data acquisition and monitoring, system automation and control, and energy efficiency. His research interests include embedded systems design, electronics, sensor and control systems in robotics, wireless sensor networks in general, and the Internet of Things.